*Progress In Electromagnetics Research Letters, Vol. 94, 19–25, 2020*

# A Method for Planar Phased Array Calibration

**Yangyi Lu*, Lei Zhou, Mantang Cui, Xiaodong Du, and Yongjun Hu**

**Abstract**—A method is proposed to calibrate a planar phased array by reconstructing its aperture distribution, in which the aperture distribution is superposed within the physical range of radiating element. Consequently, the calibration coefficients are solved for the linear relationship between the superposed aperture distribution and elements' excitations. The calibration accuracy that is influenced by resolution of aperture distribution is also discussed in this paper. In practice, the reconstruction procedure of aperture distribution is based on the plane wave spectrum (PWS) theory, utilizing FFT and IFFT techniques. This method turns out to be valid by experiment.

## 1. INTRODUCTION

Phased array calibration ensures good performance of the array. The evaluation of the excitation of each radiating element is a fundamental part of calibrating phased array. Many phased array calibration methods have been developed in the past decades, e.g., rotating element electric field vector (REV) [1, 2], phase toggling method (PTM) [3, 4], mutual coupling method (MCM) [5, 6], and matrix method (MM) [7, 8], and some of them are based on near field measurement system. Many calibration methods need to use phase shifters of a phased array, and the effectiveness of the methods is influenced by the performance of phase shifters greatly. To get rid of the restriction, this paper proposes a calibration method based on planar near field (PNF) measurement system. The theoretical development of planar near field antenna measurements is usually based on the plane wave spectrum (PWS) representation of electromagnetic waves. For most application, the near field data are processed through Fourier transform to obtain PWS and the far field pattern of the antenna under test (AUT). Besides, near field data can be treated by "backward" transform to reconstruct the aperture distribution as a calibration method [9, 10].

The backward transformation method (BTM) is also called microwave holographic metrology. It recovers the aperture distribution in front of the array with the measured planar near field data by using the PWS theory. The resolution of reconstructed aperture distribution is equal to the sampling interval of the measured plane because of the characteristic of Fourier transform. In conventional BTM, the amplitude and phase are extracted from the reconstructed aperture at element's position. In this paper, the Fourier interpolation formula is introduced to increase the resolution of aperture distribution, then the amplitude and phase of the superposed aperture distribution in front of radiating elements are regarded as the excitation of the elements. Particularly, this paper will present the experimental results of the $45 \times 1$ microstrip patches array on planar near field system.

## 2. ANALYSIS

The calibration coefficient is derived from the aperture distribution in front of planar phased array, which can be reconstructed from the near field data through BTM. Firstly, the planar near field data

*Received 1 September 2020, Accepted 14 October 2020, Scheduled 18 October 2020*
* Corresponding author: Yangyi Lu (lyy_csic@163.com).
The authors are with the 724th Research Institute of CSIC, Nanjing 21000, China.

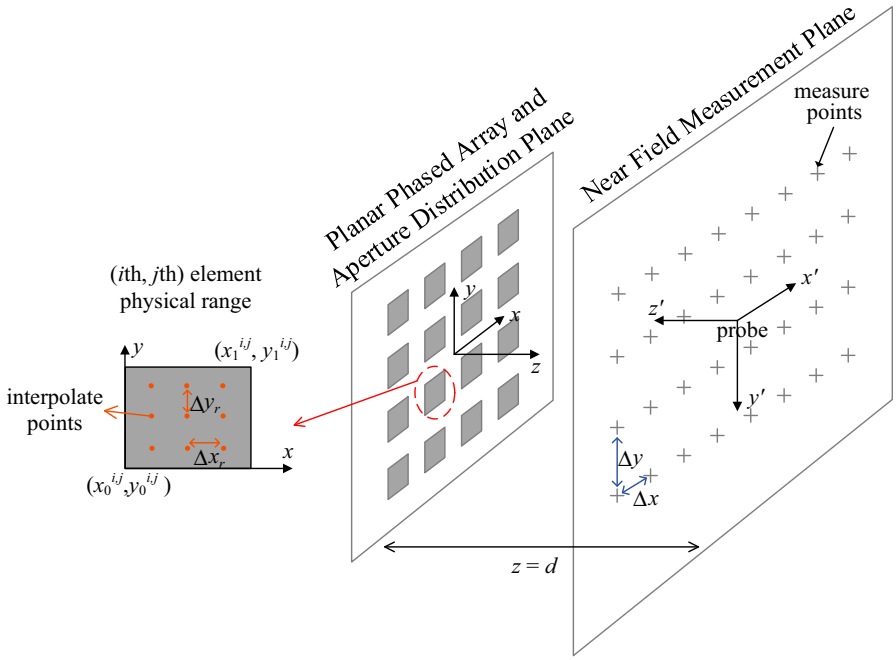


**Figure 1.** Geometry for formulation of aperture reconsctruction.

are processed through 2D Fourier transform to obtain PWS in the wave number ($\mathbf{k}$) space. After making a probe correction, an inverse transform is taken to rebuild the aperture distribution. The process of backward transform effectively translates the measurement plane from $z = d$ to $z = 0$, where the aperture field is projected as illustrated in Figure 1. Then, a Fourier interpolation formula is used to increase the resolution of the aperture distribution. Finally, the calibration coefficient is calculated from superposed electric field, which is the superposition of the interpolated aperture distribution in the element's physical range. Figure 1 shows the physical range of $(i, j)$th radiating element and sketch of Fourier interpolation, which would increase resolution of aperture distribution from $\Delta x$, $\Delta y$ to $\Delta x_r$, $\Delta y_r$.

As described in [12], the PNF scan plane is spaced approximately three wavelengths from the array. The probe output at each probe position in the scan is contributed by all the plane wave components received by the probe, which is characterized by a vector receive pattern $\mathbf{S}(-\mathbf{k})$, and the output can be written as

$$P_0(x, y, z = d) = \int_{-\infty}^{+\infty} \int_{-\infty}^{+\infty} \frac{k_z}{k} \mathbf{A}(\mathbf{k}) \cdot \mathbf{S}(-\mathbf{k}) e^{-jk_z d} e^{-j(k_x x + k_y y)} dk_x dk_y \tag{1}$$

where vector $\mathbf{A}(\mathbf{k})$ is the plane wave spectrum of AUT, and $e^{-jk_z d}$ is a spatial phase factor referred to measurement plane for a particular component specified by $k_z = \sqrt{k_0^2 - k_x^2 - k_y^2}$. It is remarked that for those components with $k_x^2 + k_y^2 > k_0^2$, $k_z$ becomes imaginary, and the wave is highly attenuated. The energy contained in those spectrum components is usually very small. In order to simplify the Equation (1), denote

$$I = \frac{1}{4\pi^2} e^{jk_z d} \frac{k}{k_z} \int_{-\infty}^{+\infty} \int_{-\infty}^{+\infty} P_0(x, y, z = d) e^{j(k_x x + k_y y)} dx dy \tag{2}$$

Hence, Equation (1) can be expressed as the matrix forms

$$\mathbf{A} \cdot \mathbf{S} = I \tag{3}$$

In Cartesian coordinate system, this PWS can be obtained directly from the sampled tangential near field data using

$$\mathbf{A}(k_x, k_y, z) = \int_{-\infty}^{+\infty} \int_{-\infty}^{+\infty} \mathbf{E}(x, y, z) e^{j(k_x x + k_y y)} dx dy \tag{4}$$

The propagating electric field everywhere in the forward half-space can be obtained from the tangential PWS as

$$\mathbf{E}(x,y,z) = \frac{1}{4\pi^2}\int_{-\infty}^{+\infty}\int_{-\infty}^{+\infty}\mathbf{A}(k_x,k_y,z)e^{j(k_x x+k_y y)}dk_x dk_y \tag{5}$$

This means that if the PWS of AUT is solved from Eq. (3), the electric field $\mathbf{E}$ is ascertained by Eq. (5). According to Maxwell's equations, the wave number vector ($\mathbf{k}$) and PWS ($\mathbf{A}$) are orthogonal, which means $\nabla\cdot\mathbf{A}=0$ or $\mathbf{k}\cdot\mathbf{A}=k_xA_x+k_yA_y+k_zA_z=0$. Hence, only two components of AUT's PWS may be specified independently, with the third being fixed since $A_z=-(k_xA_x+k_yA_y)/k_z$. As required by Equation (3), two different probes are necessary to obtain the AUT's PWS. In practice, two scan sets were measured in orthogonal polarizations to allow full characterization of the polarization performance of the array through rotating probe 90 deg clockwise. The AUT coordinate system and the probe coordinate system in the two scan sets were connected by

$$\begin{aligned}\hat{x}' &= \hat{x},\ \hat{y}' = -\hat{y},\ \hat{z}' = -\hat{z}\\ \hat{x}'' &= \hat{y},\ \hat{y}'' = \hat{x},\ \hat{z}'' = -\hat{z}\end{aligned} \tag{6}$$

Hence, Equation (3) can be written in a scalar form

$$\begin{aligned}\left(S_{x'}+\frac{k_x}{k_z}S_{z'}\right)A_x+\left(-S_{y'}+\frac{k_y}{k_z}S_{z'}\right)A_y &= I_x\\ \left(S_{y''}+\frac{k_x}{k_z}S_{z''}\right)A_x+\left(S_{x''}+\frac{k_y}{k_z}S_{z''}\right)A_y &= I_y\end{aligned} \tag{7}$$

The PWS of probe $\mathbf{S}$ can be obtained directly from its far field pattern $\mathbf{f}(\theta,\phi)=\cos\theta\cdot\mathbf{S}$. After taking $\mathbf{S}$ of the two measurements sets into Eq. (7), the AUT's unknown tangential spectrum $A_x$, $A_y$ will be easily solved. This step is also called probe compensation. Finally, an inverse transform in Eq. (5) is performed to recover the aperture distribution $\mathbf{E}(x,y,z=0)$.

It should be pointed out that the effect of the probe has been considered in Equation (7). As mentioned above, when horizontal polarization measurement is taken. The PWS of probe can be derived from its far field pattern [11]

$$\begin{aligned}S_x &= f_E(\theta)\cos^2(\phi)+f_H(\theta)\sin^2(\phi)/\cos(\theta)\\ S_y &= f_E(\theta)\sin(\phi)\cos(\phi)-f_H(\theta)\sin(\phi)\cos(\phi)/\cos(\theta)\\ S_z &= -f_E(\theta)\cos(\phi)\sin(\theta)\cos(\theta)\end{aligned} \tag{8}$$

where $(r,\theta,\phi)$ is the probe's spherical coordinate system.

The array calibration ensures all radiating elements of the array working at equal amplitude and phase condition. In other words, the excitation of all elements should be adjusted to the same amplitude and phase by using coefficient. For conventional BTM, the amplitude and phase coefficients are calculated from aperture distribution at one point (typically, the feed position or the center of element) relating to each element, and it will cause great error. The method proposed in this paper assumes that aperture distribution in front of radiating element are dependent on spatial position $(x,y)$ and proportionate to its excitation. It is reasonable understanding from [8]. So the superposed aperture electric field can be regarded as the excitation of radiating element

$$E^s_{i,j} = \int_{x_0^{i,j}}^{x_1^{i,j}}\int_{y_0^{i,j}}^{y_1^{i,j}}E(x,y)dxdy \propto \sum_{p=1}^{M_0}\sum_{q=1}^{N_0}\alpha_{p,q}U_{p,q} \tag{9}$$

where $U_(p,q)$ is the $(p,q)$th element's excitation of array including amplitude (or voltage) and phase. The spatial position $(x_0\sim x_1, y_0\sim y_1)$ is the $(i,j)$th element's physical range as illustrated in Figure 1. The phased array contains $M_0\times N_0$ $(i\in[1,M_0], j\in[1,N_0])$ elements. The mutual coupling coefficient is $\alpha_{p,q}=0$ $(p\neq i, q\neq j)$ and $\alpha_{p,q}=1$ $(p=i,q=j)$ due to the assumption that the current distribution at each element is not impacted by mutual coupling. $E^s_{i,j}$ is the superposition of the reconstructed aperture electric fields $E(x,y)$ in the $(i,j)$th element's physical range.

Actually, the near field measurements are performed at discrete points and 2D Fourier transform, being forward or backward, which is carried out with fast Fourier transform (FFT) techniques. The

sampling intervals should satisfy Nyquist sampling theorem, which is $\Delta x \leq \lambda/2$, $\Delta y \leq \lambda/2$. The measurement plane is divided into $M \times N$ grid points. The process of FFT or IFFT will generate the same number of data points ($M \times N$) in $\mathbf{k}$ space and aperture plane. So the resolution of aperture distribution is equal to the intervals of near field. There is an efficient algorithm to increase the aperture field resolution, which is Fourier interpolation algorithm

$$E(x,y) = \sum_{n=1}^{N}\sum_{m=1}^{M} E(m,n)\frac{\sin(m-M/2-1-x/\Delta x)}{(m-M/2-1-x/\Delta x)\pi}\frac{\sin(n-N/2-1-y/\Delta y)}{(n-N/2-1-y/\Delta y)\pi} \tag{10}$$

where $E(m,n)$ is the reconstructed aperture distribution on $(m,n)$th point of scan grid ($m \in [1,M], n \in [1,N]$), and $E(x,y)$ is the interpolated aperture distribution at spatial position $(x,y)$.

In theory, high resolution of the reconstructed aperture distribution can be achieved by formula (10), but the higher resolution results in more consumption of computing resource and time. To derive the error between excitation and superposed electric field of radiating elements, the rms errors of the amplitude and phase are defined

$$\epsilon_A = \text{std}\left(20\log_{10}\left|\frac{E^s_{i,j}}{E^s_{\max}}\right| - 20\log_{10}\left|\frac{E^e_{i,j}}{E^e_{\max}}\right|\right) \tag{11}$$

$$\epsilon_P = \text{std}\left(\text{angle}(E^s_{i,j}) - \text{angle}(E^e_{i,j})\right) \tag{12}$$

where superscript $s$ denotes the superposed electric field of reconstructed aperture distribution, and superscript $e$ denotes the excitation of radiating element. Subscript $(i,j)$ denotes the $(i,j)$th element of array. Function std denotes the standard deviation operation.

## 3. EXPERIMENT RESULT

The above formulation has been applied to the calibrated measurements of an S-band test phased array. A phased array consisting of $45 \times 1$ microstrip patches was considered to test in PNF measurement system, whose element was offset fed with 31.18 mm × 46.75 mm size. The microstrip patches lie on $XY$ plane, and the distance between adjacent elements is 50 mm. The array structure is shown in Figure 2, and the array transmitted field propagates to positive $Z$ axis. Specially, the polarization of the array in measurement configuration was horizontal ($X$ axis), and the $I_y$ in Equation (7) is zero. Therefore, only one configured measurement is needed, and there is no necessity to rotate probe for getting more near field data.

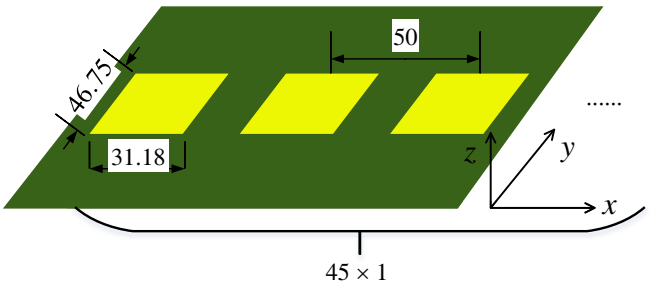


**Figure 2.** The structure of microstrip patch array.

The beam forming should be implemented in the array because only element-level PNF data are available, when the array is characterized in receiving mode. Consequently, the measurements described here relate only to data collected with the array in transmitting mode. However, this technique is not limited to the characterization of the transmitting mode for the array, but additional hardware or software would be required in receiving mode using a PNF system.

Planar near field measurements were taken at 3 GHz, at a probe distance of $z = 500$ mm over a grid of $145 \times 61$ points. The sampling intervals were $\Delta x = 0.5\lambda$ and $\Delta y = 0.5\lambda$. After processing the near field data with Eqs. (2), (7), and (5), the projected aperture distribution at $z = 0$ was

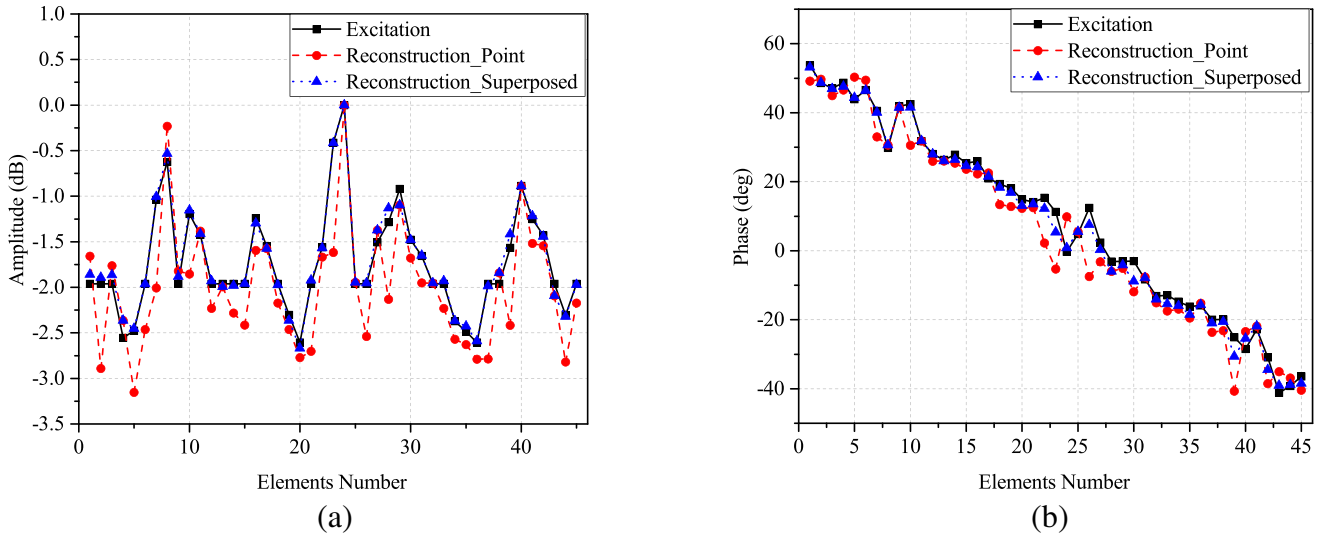


**Figure 3.** The comparison between excitation and reconstructed aperture distribution. (a) Amplitude. (b) Phase.

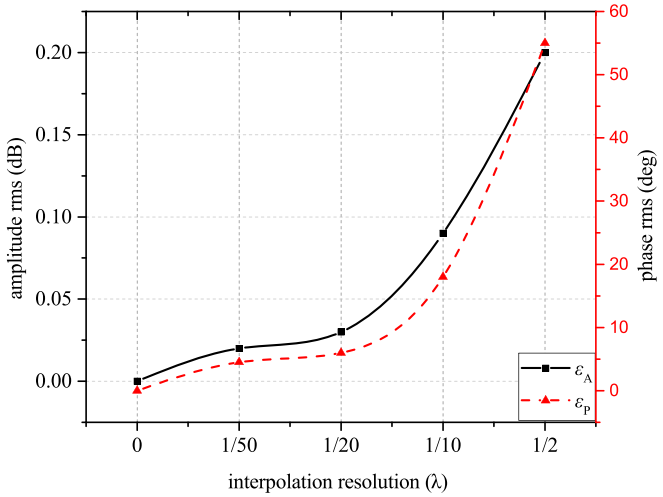


**Figure 4.** The errors of amplitude and phase influenced by interpolating space.

obtained. As mentioned in analysis section, the spatial resolution of this aperture distribution is same with $\Delta x$ and $\Delta y$ before interpolating. There was much error compared to excitation (solid line in Figure 3) by extracting aperture amplitude and phase at one point position, which is denoted as Reconstruction_Point, as the dash line presented in Figure 3. Next, using interpolation algorithm in Eq. (8) to obtain "denser" aperture distribution, the core of the method superposes the reconstructed aperture electric field in front of each radiating element's physical range. The superposed electric field is denoted by Renconstruction_Superposed, as the dot line shown in Figure 3. Apparently, the Reconstruction_Superposed curve is much closer to the excitation curve. It should be noted that the interpolation interval here is $\Delta x_r = \Delta y_r = \lambda/20$. The resolution of aperture distribution is increased from $\lambda/2$ to $\lambda/20$.

The superposed electric field in front of radiating element is regarded as the excitation of the element, which is influenced by the resolution. So the calibration accuracy is affected by the resolution directly. In the discretization of superposition integral in Eq. (9), higher resolution or smaller discrete spacing results in more accurate discrete summation. The errors of amplitude and phase under different interpolating space intervals are shown in Figure 4. When the interpolating space is greater than

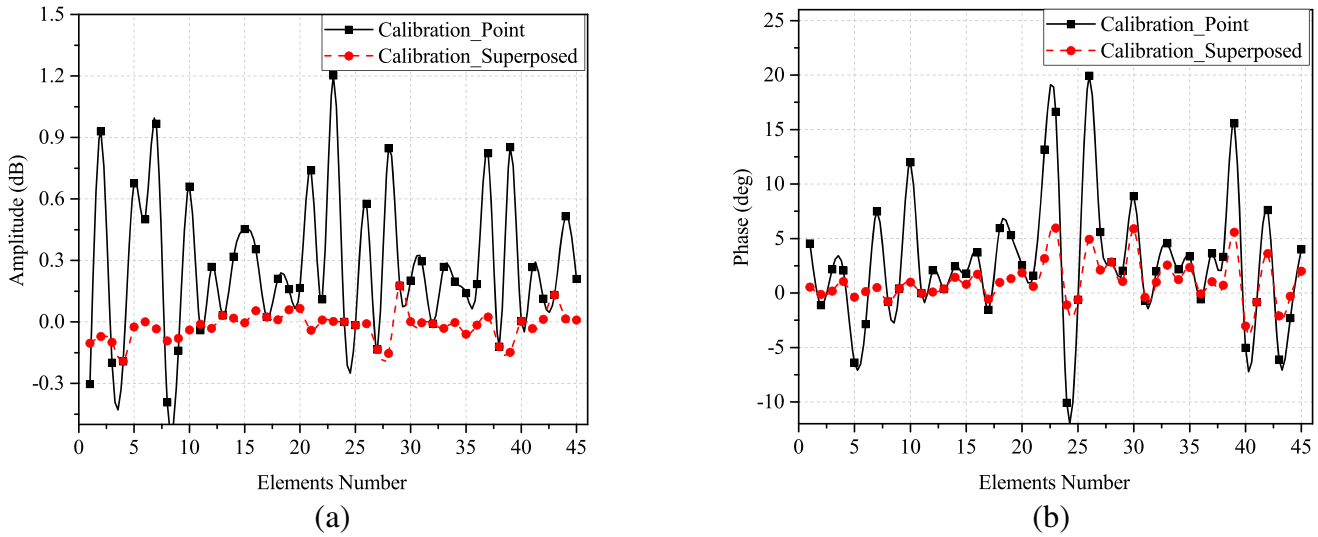


**Figure 5.** The calibration result with point and superposed reconstructed aperture distribution. (a) Amplitude. (b) Phase.

$\lambda/15$, the error increases rapidly. The spacing $\lambda/20$ is a good compromise between accuracy and the consumption of time and computational resource.

The result of calibration through Reconstruction_Point and Reconstruction_Superposed are shown in Figure 5. It is obvious that the calibration coefficient calculated from Reconstruction_Superposed ensures all elements working at equal amplitude and phase effectively.

## 4. CONCLUSION

This paper proposes a modified calibration method for planar phased array with a PNF measurement system, which is based on BTM. Compared with the traditional BTM, the superposed aperture electric field in front of radiating elements has higher accuracy, when the resolution of reconstructed aperture distribution is less than $\lambda/20$. It is confirmed to be valid by experimental results.

## REFERENCES

1. Mano, S. and T. Katagi, "A method for measuring amplitude and phase of each radiating element of a phased array antenna," *Electronics and Communications in Japan*, Vol. 65, No. 5, 1982.
2. Takahashi, T., H. Miyashita, Y. Konishi, et al., "Theoretical study on measurement accuracy of rotating element electric field vector (REV) method," *Electronics and Communications in Japan*, Vol. 89, No. 1, 2006.
3. Lee, K. M., R. S. Chu, and S. C. Liu, "A built-in performance-monitoring/fault isolation and correction (PM/FIC) system for active phased-array antennas," *IEEE Transactions on Antennas and Propagation*, Vol. 41, No. 11, 1530–1540, 1993.
4. Hampson, G. A. and A. B. Smolders, "A fast and accurate scheme for calibration of active phased-array antennas," *IEEE International Symposium on Antennas and Propagation*, 1040–1043, Orlando, 1999.
5. Aumann, H. M., A. J. Fenn, and F. G. Willwerth, "Phased array antenna calibration and pattern prediction using mutual coupling measurement," *IEEE Transactions on Antennas and Propagation*, Vol. 37, No. 7, 844–850, 1989.
6. Gu, Q., C. Dai, C. Zhang, et al., "Analysis of amplitude-phase error of phased array calibration in mid-field," *Asia-Pacific Conference on Antennas and Propagation*, 280–283, Harbin, 2014.

7. Bucci, O. M., D. Migliore, G. Panariello, et al., "Accurate diagnosis of conformal arrays from near-field data using the matrix method," *IEEE Transactions on Antennas and Propagation*, Vol. 53, No. 3, 1114–1120, 2005.
8. Long, R. and J. Ou Yang, "Planar phase array calibration based on near-field measurement system," *Progress In Electromagnetics Research C*, Vol. 71, 25–31, 2017.
9. Hanfling, J. D., G. V. Borgiotti, and L. Kaplan, "The backward transform of the near field for reconstruction of aperture fields," *Proc. IEEE Antennas Propagat. Symp.*, Vol. 2, 764–767, 1979.
10. Lee, J. J., E. M. Ferren, D. Pat Woollen, et al., "Near-field probe used as a diagnostic tool to locate defective elements in an array antenna," *IEEE Transactions on Antenna and Propagation*, Vol. 36, No. 6, 884–889, 1988.
11. Yaghjian, A. D., "Approximate formulas for the far field and gain of open-ended rectangular waveguide," *IEEE Transactions on Antenna and Propagation*, Vol. 32, No. 4, 378–384, 1984.
12. Gregson, S., J. McCormick, and C. Parini, *Principles of Planar Near-field Antenna Measurements*, The Institution of Engineering and Technology, London, United Kingdom, 2007.